Journal of Natural Gas Science and Engineering 35 (2016) 468–482

Contents lists available at ScienceDirect

Journal of Natural Gas Science and Engineering

journal homepage: www.elsevier.com/locate/jngse

Investigation on the permeability characteristics of bedded salt rocks and the tightness of natural gas caverns in such formations

Wei Liu [a, b, d], Nawaz Muhammad [c, e], Jie Chen [a, b, d, *], C.J. Spiers [c], C.J. Peach [c], Jiang Deyi [a, b, **], Yinping Li [a, d]

[a] State Key Laboratory of Coal Mine Disaster Dynamics and Control, Chongqing University, Chongqing, China
[b] College of Resources and Environmental Science, Chongqing University, Chongqing, China
[c] High Pressure and Temperature Laboratory, Department of Earth Sciences, Utrecht University, Utrecht, The Netherlands
[d] State Key Laboratory of Geomechanics and Geotechnical Engineering, Institute of Rock and Soil Mechanics, Chinese Academy of Sciences, Wuhan, Hubei, China
[e] Centre for Advanced Studies in Physics, GC University, Lahore, Pakistan

ARTICLE INFO

Article history:
Received 7 April 2016
Received in revised form
27 July 2016
Accepted 29 July 2016
Available online 1 August 2016

Keywords:
Bedded salt rocks
Natural gas cavern
Permeability
Interface
Gas seepage
Tightness

ABSTRACT

In China, the salt formations close to the lower reaches of the large natural gas routes and the main gas consuming regions are all bedded structures. The presences of non-halite or low-halite mudstone interlayers and interfaces (salt-interlayer) in these bedded salt formations increase the concern on the tightness of the natural gas caverns constructed in such formations. Therefore, different lithotypes of samples of bedded salt rocks have been prepared to determine their gas permeability evolution by steady-state and transient pulse-decay methods. The results show that the permeability of the samples is very low, within the range of 10^{-17} to 10^{-21} m^2 after well compacted. The permeability of the interface is comparatively the highest, steadily around the order of 10^{-17} m^2. A similar tendency of reducing permeability as deviatoric stress increases is found for all the samples; and unexpectedly there is no dilatancy and consequently steep increase of the permeability for all samples, even under very high differential stress. SEM (scanning electron microscopic) testing, as a supplement of tightness assessment, shows tight microstructure of all the bedded salt rocks cores. The experimental results indicate favourable performances for the tightness of natural gas caverns in such formations. Gas seepage around a gas cavern in such bedded salt formation was simulated by the FLAC^{3D} software over a lifespan of 30 years. The results present that the interfaces act as the main channels for the gas to seep through. But the seepage distances in the vicinity of the cavern are so short that it causes a little influence on the tightness. Several factors, e.g., the internal gas pressure, the locations of interface, as well as the permeabilities of the interlayers were analyzed to investigate their effects on the tightness of a gas cavern. On the whole, the bedded salt rocks have enough low permeability and satisfactory tightness for the natural gas caverns constructed in.

1. Introduction

Natural gas consumption changes seasonally and periodically, so that the storage of gas plays a vital role to maintain the stability of the gas market (Jong, 2015). To ensure the sustainable supply of natural gas, more than 36 countries constructed their own gas storage facilities. In both the North-America (US + Canada) and Europe (OECD countries) the natural gas storage capacity measured by working volume is approximately 18% of the total annual consumption (International Energy Association, 2012). Due to the high safety margin (effectively avoiding accidents such as those due to lightning, war and terrorist attacks, etc.), lower cost and less occupation of land, underground storage facilities have much more extensive utilizations compared to the aboveground steel/concrete tanks (Li et al., 2012). With the rapid development of the economy, the total consumption of natural gas of China was 1800 × 10^8 m^3 in

* Corresponding author. State Key Laboratory of Coal Mine Disaster Dynamics and Control, Chongqing University, Chongqing, 400044, China.
** Corresponding author. College of Resources and Environmental Science, Chongqing University, Chongqing, 400044, China.
E-mail addresses: chenjie_cqu@163.com (J. Chen), deyij@cqu.edu.cn (J. Deyi).

http://dx.doi.org/10.1016/j.jngse.2016.07.072
1875-5100/

2014, and will rise to 2340 × 10^8 m^3 in 2020 (Wang et al., 2015a). However, up to now, the total amount of the natural gas stock is only 56 × 10^8 m^3 in China, as low as 3% of the annual consumption. Thus, for the China government, to construct more underground gas storage facilities has become an urgent duty to ensure the natural gas market.

Three main geological formations are available for the underground natural gas storage, namely depleted oil/gas reservoirs, aquifers and salt caverns. The depleted oil/gas reservoirs generally exhibit the largest working volume but need a high proportion of cushion gas, and the withdrawal efficiency of them is low, as do aquifers. In addition, in East and Central China, where close to the middle and lower reaches of the large gas transmission routes (West-East Gas Transmission and Sichuan to East Gas Transmission) or close to the primary consumption markets (Yangtze River Delta region), there is a lack of depleted oil/gas reservoirs and aquifers but are abundant of large-scale salt formations in underground, which provides an alternative to build large-scale underground gas storage caverns in these salt beds (Zhang et al., 2014).

Rock salt is characterized by the low porosity and permeability, marked plasticity as well as capacity of self-healing when damaged. Thus, it is recognized as the best host rock to store crude oil and natural gas (Johnson and Seni, 2011; Yang et al., 2015). For instance, by the end of 2005, 198 × 10^8 m^3 natural gas was stored in salt caverns in Germany, 100 × 10^8 m^3 in France and 112 × 10^8 m^3 in Italy; In the USA, 23% of underground natural gas storage caverns were constructed in salt formations in 2011 and the proportion tends to increase continuously (Wang et al., 2015a). The China government plans to establish 5 huge natural gas storage sites in salt formations in central and eastern China by the end of 2020, the total storage volume of which will be as large as 4 × 10^7 m^3 (Yang et al., 2009).

Abroad, natural gas storage caverns are mainly constructed in marine deposit domal salt or thick salt formations (Staudtmeister and Rokahr, 1997; Hou, 2003). These types of salt beds have thick salt layers, homogeneity of components and low proportion of impurities. In such salt beds, the size of the caverns is often very large, usually 200–500 m in height, and up to 1,000,000 m^3 in volume (Fig. 1-a). However, the salt beds in China are typically thinly layered structures. These salt beds are characterized by complex tectonic structures, numerous interlayers and high impurity content (Li et al., 2012; Zhang et al., 2014; Yang et al., 2009, 2015), as visualized in Fig. 1-b. The higher proportion of impurities changes the composition and texture of the rock salt, but little is known about their effect on the permeability. The non-halite or low-halite interlayers often consist of anhydrite, argillaceous rocks, glauberite and shale, which usually have higher porosity and permeability as compared with rock salt (Zhou et al., 2009; Xiong et al., 2015). Their impacts on the tightness of the wall rock are also unknown. Moreover, bedded salt rock, as a typical composite material, stress concentration will form along the interface due to the unmatched deformations of the rock salt and interlayer near the interface (Li et al., 2014). Once the stress concentration exceeds the threshold shear strength of the interface, cracks will initiate and propagate, and hence induce slippage between the adjacent layers, and consequently results in percolation channels along the interface (Li et al., 2014; Muhammad et al., 2015). This will cause adverse effects on the tightness and stability of the storage caverns. Therefore, for the gas caverns in bedded salt rocks, the permeability of interlayer and interface as well as their influence on the tightness of the cavern are of utmost importance to be investigated.

For the permeability characteristics of relatively pure rock salt from domal salt, many studies from both the laboratory measurements and field surveys have been implemented (Hunsche, 1996; Alkan, 2009; Stormont, 1997; Consenza et al., 1999). Among all the studies, the damage criterion of the compression-dilatancy boundary (CDB) of the rock salt has been widely utilized for the cavern design and safety assessment (Hunsche, 1996). However, with regard to the permeability of the bedded salt rocks and the tightness of gas caverns in these strata, the studies seem too scarce to provide adequate guidance for engineering applications. Zhou et al. (2009) presented permeability tests on pure salt rock and anhydrite rock salt, they found that the rock salt has a permeability range between 10^{-16} m^2 and 10^{-18} m^2, but the anhydrite rock salt is almost impermeable. Xiong et al. (2015) revealed the gas seepage distance around a cavern in bedded salt rock but supplied no support of parameters from laboratory measurements. Adopting the steady-state method by using nitrogen as a permeant, Liu et al. (2015) conducted permeability measurements on mudstone cap rock and interlayers, taken from a pilot-well in Jintan Salt Mine, eastern China, which supplies some references for the tightness assessment of caverns in such salt formations. The interface that connects the adjacent rock salt and interlayer is a significant structure to greatly influence the tightness of a salt cavern. Although more attention is focussed on the permeability and evolution of the interface, due to the limitations of available cores, coring technique, and low-permeability testing technologies, the studies on the permeability of bedded salt rocks and its reaction to variable deviatoric stress, particularly the permeability characteristics of the interface, are still stagnant.

To solve the lack of knowledge about the permeability properties of the bedded salt rocks as well as the extreme lack of tightness

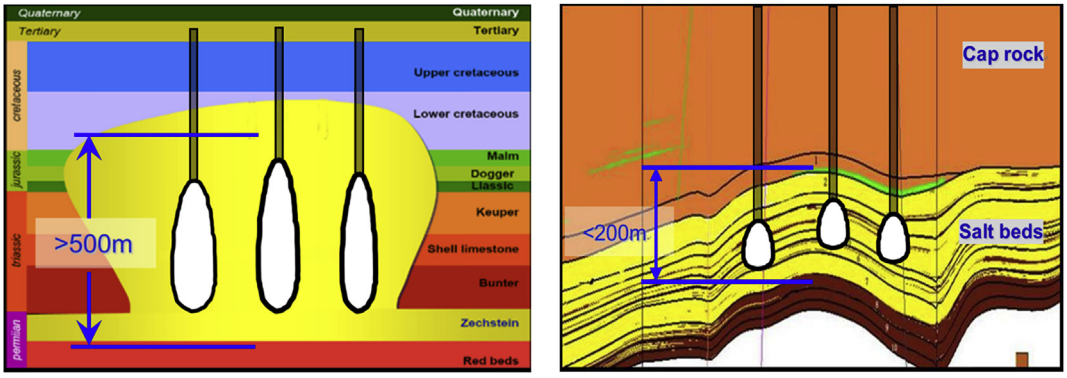

(a) Storage caverns in salt dome

(b) Storage caverns in bedded rock salt

Fig. 1. Comparison of caverns, respectively located in a domal salt and in bedded salt rocks.

assessment for gas cavern in such formations, in this study, at first, the steady-state and transient pulse-decay pressure methods are employed to determine the permeability characteristics of the mudstone interlayer, rock salt and interface (rock salt part connected with mudstone part). And then, the permeability and its response to differential stress are measured. In the end, followed by a 3D-numerical simulation software FLAC^{3D} (Itasca, 2005) by adopting the laboratorial test results, the gas migration around a gas storage cavern in a bedded salt deposit, including seepage distance, pore pressure distribution as well as the influences of several factors on the tightness of the gas cavern are investigated and discussed. This study not only indicates the value and evolution of the permeability of the bedded salt rocks, but also supplies significant references for the tightness assessment of gas caverns in such salt beds. As a supplement and for consistency of study, we set 'rock salt' to refer to pure salt layer, 'bedded salt rocks' to refer to composite cores consisting of rock salt layers and mudstone interlayers, and 'interface' to refer to a composite sample connecting the rock salt part and mudstone part.

2. Basic theory of the permeability testing

In petroleum geology, mudstones form approximately 70% of all cap rock units, but it does not conclude that all mudstone formation acts as an effective seal bed. For instance, Yang and Aplin (2010) showed that the permeability of argillaceous rocks ranges over 6 orders of magnitude due to the differences of mineral compositions and microstructures. Even though the interlayers intersecting the caverns are mudstones, the determination of their permeability to evaluate the tightness of the cavern is still needed.

We adopted the steady-state flow method to measure the permeability of the mudstone interlayers. The lowest value that this technique can measure is approximately 10^{-20} m^2, which satisfies the accuracy requirement of the tests. For the details of the measurements and results, please refer to our previous work in reference (Liu et al., 2015).

2.1. Basic principle of pulse-decay pressure method

Under undisturbed or well compacted state, rock salt usually has a permeability as low as 10^{-20} m^2 to 10^{-22} m^2 (Alkan, 2009; Peach and Spiers, 1996). The seepage of fluid in rock salt is characterized with typical non-Darcian behaviour. For extremely low-permeability rocks, such as rock salt and anhydrite, the time until the flow becomes steady is too long to be endured in laboratory testing. Therefore, the steady state flow method of permeability testing is rarely used for extremely low permeability materials. However, for the transient pulse decay method, it is not necessary for the gas flow to become steady before measuring the flow rate, thus the testing time will be much shortened. Due to such a notable advantage, this method is extensively utilized for low permeability rock masses and so is adopted to measure the permeability of the rock salt and interface samples.

The transient pulse decay method was initially proposed by Brace and Martin (1968). The procedures of this method can be described by the following steps: 1) before testing, emplace the sample in between the upstream and downstream reservoirs, remove the air molecules by proper evacuation of the sample and flush with permeant fluid (argon gas in this case), then apply the same constant pressure on the upstream and downstream reservoirs and wait till all pores of the sample are filled and equilibrium is reached; 2) apply a pressure pulse on the upstream reservoir. Due to the pressure gradient ($\Delta P_0 = P_{up} - P_{down}$) on two sides of the sample, the pressure of the upstream reservoir (P_{up}) gradually decays, and the pressure of downstream reservoir (P_{down}) gradually rises till the pressure reaches a new equilibrium state inside the sample; 3) calculate the permeability according to the gas pressure decay principle. Fig. 2 shows the schematic diagram of this method.

2.2. Permeability calculation

Walder and Nur (1986) stated that the decline of the gas pressure in the rock sample obeys the following power function

$$\Delta P(t) = (\Delta P_0)\mathrm{e}^{-\alpha t} \tag{1}$$

where, ΔP(t) is the gas pressure difference at time "t", with unit Pa; t is testing time, with unit s; α is a constant determined by the sample sizes and testing conditions as

$$a = K\frac{A}{l}\frac{V_1 + V_2}{V_1 V_2}\frac{1}{mb} \tag{2}$$

where, κ is the permeability with unit m^2; A is the cross-sectional area of the sample facing gas stream with unit m^2; l is the length of sample with unit m; V_1 and V_2 are the volumes of upstream and downstream reservoirs respectively, with unit m^3; μ is the dynamic viscosity coefficient of Ar gas under constant temperature, with unit Pa s; β is the compressibility of Ar, with unit Pa^{-1}.

Then the permeability expression of the pulse method can be deduced as

$$\kappa = \frac{\mathrm{d}}{dt}\left[\ln\left(\frac{\Delta P}{\Delta P_0}\right)\right]\frac{l}{A}\frac{V_1 V_2}{V_1 + V_2}\mu\beta \tag{3}$$

2.3. Klinkenberg correction

For comparatively lower permeability (<10^{-19} m^2), the measured value can be higher than the absolute value (Klinkenberg, 1941), if the permeant fluid exhibits non-Darcian behaviour. This is because the flow velocity of the gas molecules will not be zero adjacent to the inner surface of a seepage channel, which will result in the gas permeability being higher than the liquid permeability (absolute permeability). Only when the pore radius approaches the mean-free-path of the gas molecules, will such a micro mechanism appear. So, when gas is employed as a permeant for low permeability rocks, the permeability should be modified by the Klinkenberg equation (Klinkenberg, 1941).

Zhou et al. (2009) stated that the gas permeability is about 30–50% higher than the absolute permeability for bedded rock salt. Peach and Spiers (1996) indicated that gas pressure is a significant factor that influences the Klinkenberg effect. When the mean gas pressure is higher, the slippage effect will become smaller. This is easily explained: the higher the mean gas pressure, the smaller the mean-free-path, and thus the smaller the slippage effect. In this study the mean pressure is set to be greater than 1.5 MPa to overcome the slippage effect.

3. Preparations for the measurements

3.1. Sample preparation

The cores of bedded salt rocks were taken from Jintan Salt Mine, at a depth range of 870–1100 m. The bulk has dark and light texture visible, and contains obvious halite grains (Fig. 3). The interlayers consist of glauberite mudstone, saline mudstone and anhydrite mudstone. The interfaces that connect the rock salt layer and interlayer also have different visual morphologies, presenting

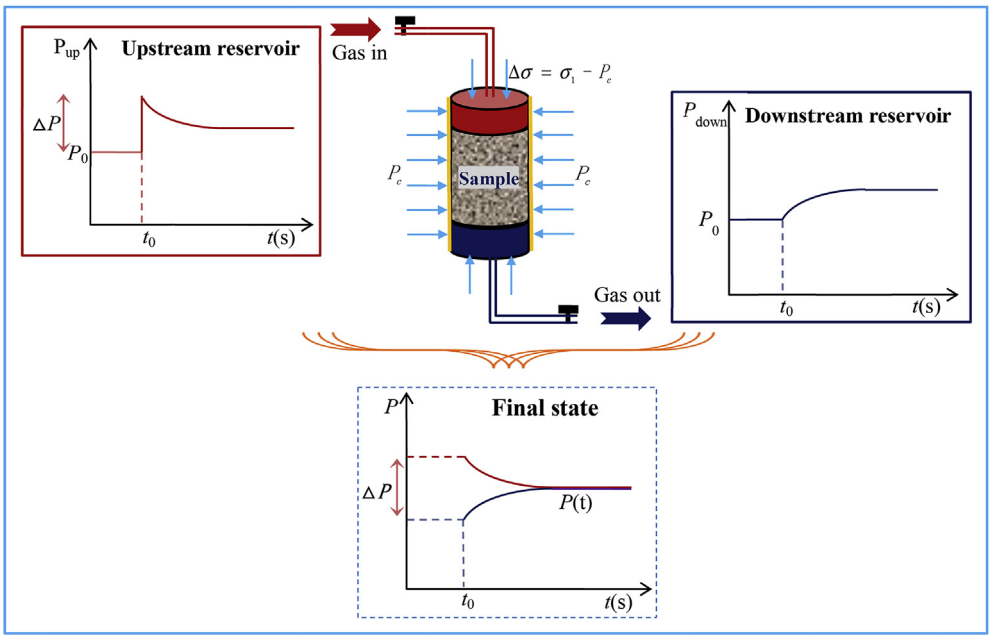

Fig. 2. Schematic sketch of the transient pulse decay method.

Fig. 3. A typical image of the rock salt cores (core diameter = 100 mm).

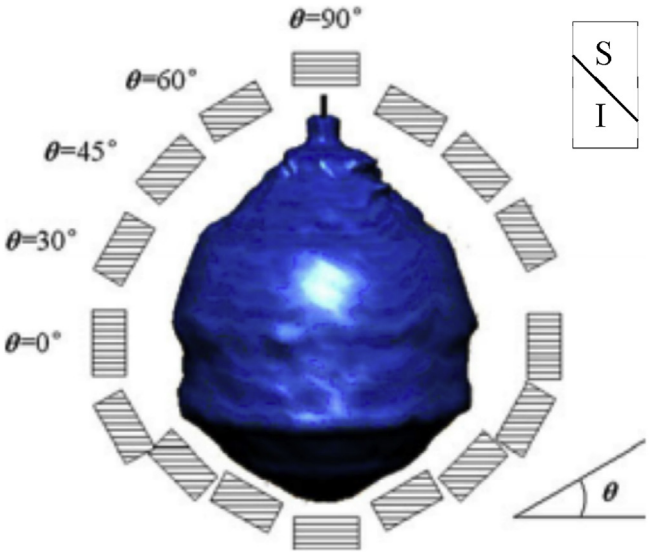

Fig. 4. Orientation of the interface plane changes with respect to the principal stress orientation around the cavern in bedded salt formation (θ: angle from σ_1 to interface plane, S: rock salt, I: interlayer) (Cited from reference Zhang et al. (2014)).

different sedimentary environments and different tectonic activities. Zhang et al. (2014) indicated that after the formation of a salt cavern, the stresses in the rock wall redistributed, so the interfaces at different locations have different inclinations with the principal stresses in the rock wall (Fig. 4). To investigate the mechanical and permeability characteristics of the interface, the samples with inclined interface were prepared. The inclined sample has the advantage that there exists shear stress on the inclined interface, which is effective to reflect how the permeability evolves when subjected to different shear stress. For comparison, rock salt samples were also prepared.

The cores of the bedded salt rocks are approximately 100 mm in diameter. The samples for laboratory testing are generally 50 mm or 25 mm in diameter, and have a ratio 1: 2 of the length to diameter. Rock salt is soluble in water and has typical crystal structure, so it is prone to crack under a mechanical disturbance. Both water drilling and dry drilling are unsuitable to fabricate the rock salt samples. The same is true for the mudstone interlayers, as they contain clay minerals (expanding when contacting water) and soluble compositions (NaCl, Na_2SO_4, etc.). Therefore, for the sample containing an interface, it is difficult to prepare for laboratory testing by sophisticated machinery. The samples were then prepared using a hand saw and grinding papers to acquire the required different orientation of the interface to differential stress of testing. The schematic diagram, showing different stages of sample preparations, is shown in Fig. 5.

Typical prepared samples are shown in Fig. 6.

As seen in Fig. 6, the sample of 3-1-1 is pure rock salt, with transparent in colour, the grains are irregular in shape with approximately 10 mm in diameter. The sample 1-47 is a mudstone rock salt, which is cored from a transition region that connects a mudstone interlayer and a rock salt layer. The sample consists of an impurities rich part and a halite rich part. And an indistinct inclined interface locates in the center in axis-direction. In the whole, this sample has a high content of impurities (>25%). Two holes on each

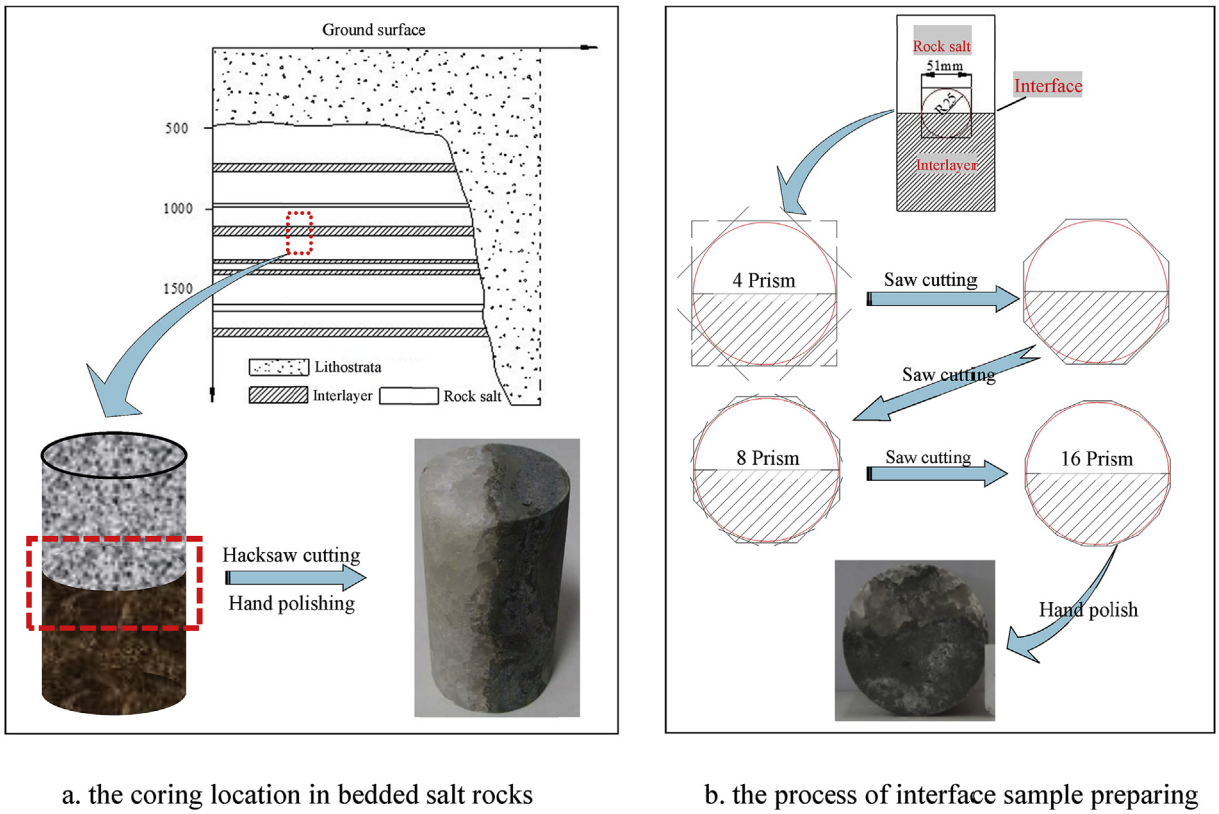

Fig. 5. Schematic diagram of a sample preparation sequence.

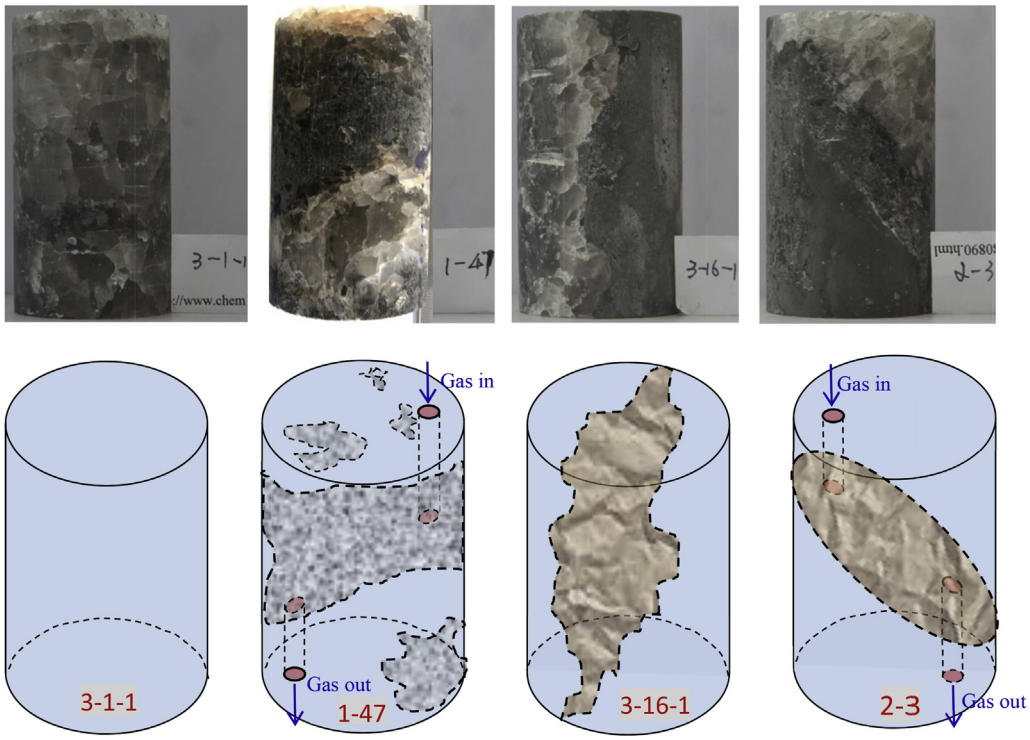

Fig. 6. Samples prepared for testing: first row: the pictures show pure rock salt (halite>95%), mudstone-rock salt (halite<75%), inclined interface, and horizontal interface, respectively; second row: mudstone rich part of Sample 1-47, inclined interface in Sample 2-3 and horizontal interface in Sample 3-16-1, respectively.

ends of the sample were drilled to induce gas flow through the 'inclined interface'. The Sample 3-16-1 is a vertical interface. The interface is oven in shape and the argillaceous part and the rock salt part seem well combined. The Sample 2-3 contains an inclined interface, the inclination of which is approximately 45°. The purpose of making such an inclined interface is to guide shear stress and unmatched deformation along the interface. Two holes on each ends were drilled to induce the gas flow through the interface. The dimensions and petrophysical information of the samples are listed in Table 1.

3.2. Permeability testing of mudstone interlayers

The steady-state flow method was used to measure the permeability of the mudstone interlayer. According to our previous studies (Liu et al., 2015), under the confining pressure of 2.5 MPa, the permeability is around 10^{-16} m^2; whereas under the confining pressure of 5 MPa–10 MPa, the permeability of the interlayer is in range between 6.23×10^{-18} m^2 and 1.21×10^{-20} m^2. The initial permeability is as high as 10^{-16} m^2, which may be related to the initial damage caused by coring damage, stress release and internal-cracks reopening. The applied confinement significantly affects the permeability. The higher the applied confining pressure, the lower the permeability will be. Permeability decreases about 2 orders of magnitude when the confining pressure is up to a certain "Compression threshold pressure". Compared to the stress state in the rock wall of a cavern depth, the permeability of the interlayer, when beyond the 'Compression threshold pressure', can well represent the permeability in the vicinity of a storage cavern, that is the permeability will be around 10^{-18} m^2 or lower.

3.3. Permeability testing of rock salt

The pulse-decay pressure method was applied to measure the permeability of the rock salt and interface. The permeant used is argon gas (*Ar*). The testing is conducted by combining a triaxial compression cell and permeability equipment at the High Pressure and Temperature (HPT) laboratory of the University of Utrecht. For more information of the apparatus, please refer to our previous study (Peach and Spiers, 1996). The mean *Ar* gas pressure is 1.5 MPa. For all the samples, in the initial stages, the permeability testing was conducted under the confining pressure state of between 5 MPa and 20 MPa, the purpose of which is to acquire the permeability of the samples under undisturbed conditions, and also to compact the cracks and simulate the near in situ condition. For a general mechanical instrument, before the differential stress ($\Delta\sigma = \sigma_1 - \sigma_3 = \sigma_1 - P_c$) exceeds zero, the axial stress (σ_1) equals the confining pressure (P_c). Thus, for the whole process of the confining pressure ($\Delta\sigma = \sigma_1 - P_c = 0$) loading, we use hydrostatic stress to describe the stress state the sample undergoes the real stress state that the sample undergoes. When the differential stress exceeds zero, we use confining pressure. After the whole process of hydrostatic stress state, keeping the confining pressure as 20 MPa, and applying the differential stress was applied at a deformation rate of ~10^{-5} s^{-1}, with incremental steps of 10 MPa to reach to a maximum value of 40 MPa, and the permeability of the samples was measured at each step by arresting the deformation piston of triaxial apparatus. The sample was then completely unloaded and the permeability was measured again under the hydrostatic pressures of 20 MPa and 5 MPa respectively.

4. Permeability testing results of rock salt and interface

4.1. Permeability investigation of rock salt

4.1.1. Permeability evolution of pure rock salt (sample 3-1-1)

For the pure rock salt sample, at the beginning, when the hydrostatic pressure is 5 MPa, the corresponding permeability is as high as 1.46×10^{-16} m^2, which is almost 4 to 5 orders of magnitude higher than that of well-compressed rock salt (Alkan, 2009; Stormont, 1997). This indicates that the dislocation and slippage between grains of the rock salt and damage occurred. After increasing the hydrostatic pressure to 20 MPa, the permeability reduces to 6.00×10^{-17} m^2, indicating the compression has induced a certain reclosing of the microcracks as well as reduced the connectivity. After applying the differential stress ($\Delta\sigma = \sigma_1 - \sigma_3$), the permeability further decreased. For a differential stress of 10 MPa, the permeability decreased to 1.29×10^{-17} m^2. And with further deformation to 20, 30 and 40 MPa, the permeability dropped below the testing accuracy (10^{-21} m^2) of the device.

As per mechanical data shown in (Fig. 7-a), the sample did not dilate but compacted as the volumetric strain is negative. The permeability of the sample as response to confinement and differential loading is shown in (Fig. 7-b). This suggests that the threshold condition for the dilatancy of the pure rock salt and consequently the increase of permeability needs further straining beyond 40 MPa. With respect to engineering application, this is a relevant property for the tightness and stability of the natural gas storage salt cavern. During the operation of a gas cavern, many types of situations may be faced. Sometimes, high deviatoric stress can take place around the cavern, due to urgent withdrawal, or at low pressure period. For these situations, the gas withdrawal rate as well as the lower limit of the gas pressure must be strictly controlled to avoid too high deviatoric stresses and dilatancy which in turn can increase the permeability of the wall rock.

After completely removing the differential load and reducing the confinement to 5 MPa, the permeability of the sample found in the impermeable range (<10^{-21} m^2), which is a value approximately 5 orders of magnitude lower than the initial permeability of the pure rock salt. This phenomenon strongly demonstrates that the deformation of the pure rock salt is irreversible, nonlinear and represents post-elastic behaviour. So, after stress unloading, the recovery of the strain (reopening of the cracks, dislocation and slippage of the grain boundaries due to unloading) lags much behind the stress. In a short period, the micro-texture of the rock salt will not be disturbed showing an obvious damage, and the permeability will not increase in a short period. It is a useful result for engineering practice. If an urgent gas withdrawal has to be conducted during the service periods of a gas cavern, from the viewpoint of tightness, the permeability of the rock salt, by a short period withdrawal, will not increase to a higher value due to its excellent hysteretic-strain characteristic. Even so, the duration time

Table 1
Sample dimensions and petrophysical information of the samples.

Sample no.	Length (mm)	Diameter (mm)	Coring depth (m)	Lithotypes	Density (g/cm^3)	Porosity (%)
3-1-1	92.63	49.94	968.41–968.86	Pure rock salt	2.23	1.5
1-47	87.64	49.82	873.75–874.1	Mudstone rock salt	2.26	1.7
2-3	86.02	49.87	897.11–897.71	Inclined interface	2.33	1.4
3-16-1	87.50	49.75	972.74–973.25	Horizontal interface	2.44	4.5

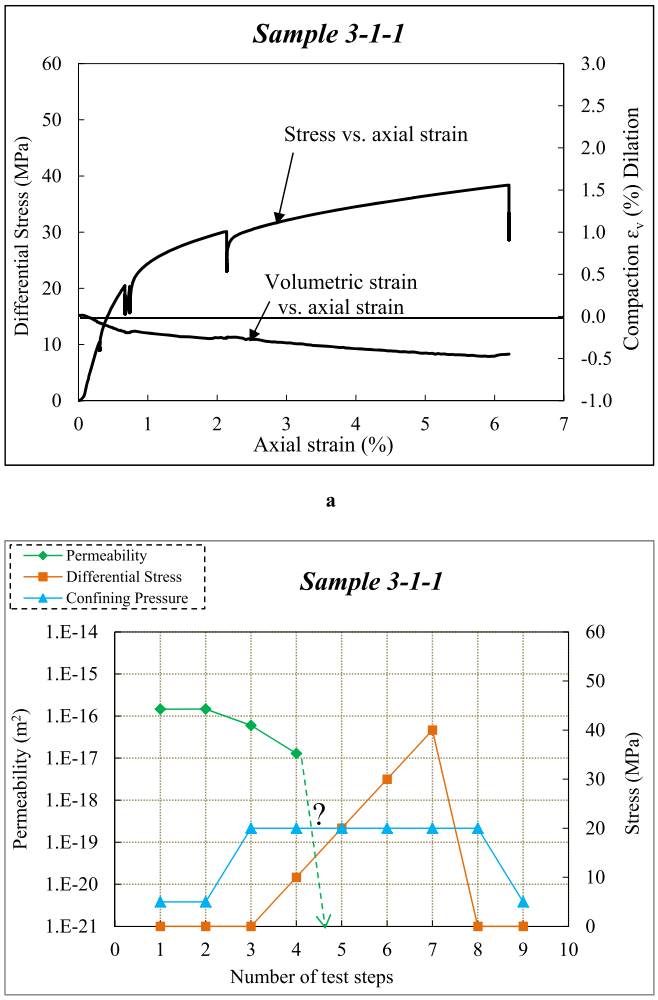

Fig. 7. Mechanical and permeability testing results of pure rock salt: Differential stress and volumetric strain vs. axial strain; (b) permeability (primary y-axis), confining pressure and differential stress (secondary y-axis) in sequence of steps.

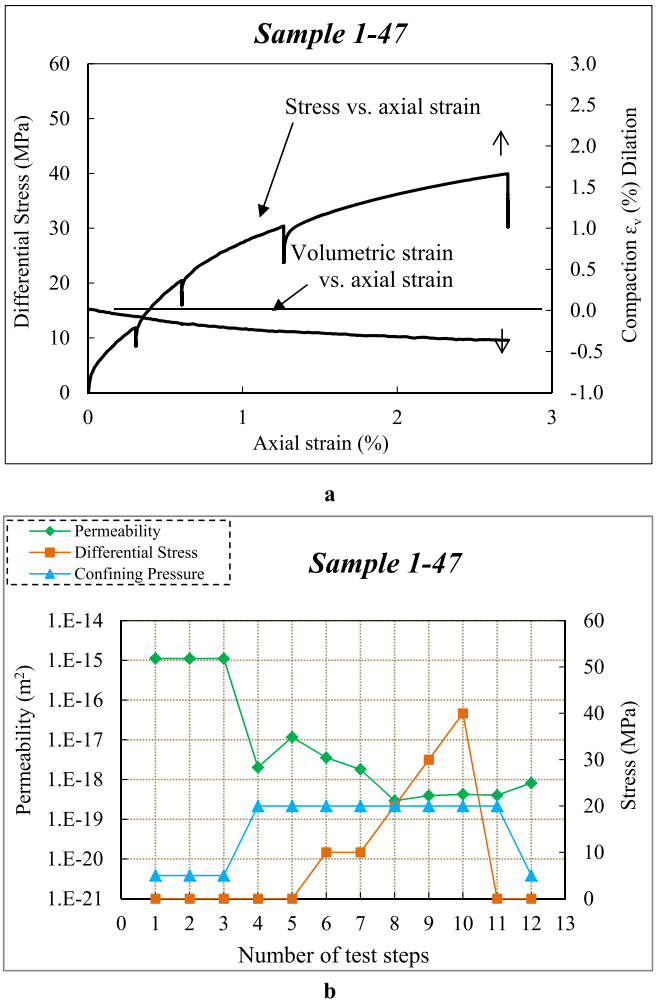

Fig. 8. Mechanical and permeability testing results of mudstone rock salt: Differential stress and volumetric strain vs. axial strain; (b) permeability (primary y-axis), confining pressure and differential stress (secondary y-axis) in sequence of steps.

of the urgent withdrawal needs to be strictly controlled and the gas injection must be implemented in time.

4.1.2. Permeability evolution of mudstone rock salt (sample 1-47)

For the mudstone rock salt (impurities $\geq$ 25%), when the hydrostatic stress equals 5 MPa, the permeability is as high as 1.11×10^{-15} m^2, almost one order of magnitude larger than that of the pure rock salt (Sample 3-1-1) under the same condition, which indicates that damage is more serious when the sample contains more impurities. When the hydrostatic pressure is raised to 20 MPa, the permeability decreases to 2.02×10^{-18} m^2, demonstrating that the micro-cracks and fissures reclose and the connectivity of voids decreases. Compared with the pure rock salt, the permeability sensitivity of the mudstone rock salt to hydrostatic pressure seems more obvious, that is, the permeability reduces by 99.8% when the hydrostatic pressure changes from 5 MPa to 20 MPa, which is higher as compared with pure salt (58.9%). With step-wise increase in differential stress (while keeping the confining pressure constant), the permeability gradually decreases till 20 MPa deformation. Beyond that, for 30 and 40 MPa, the trend slightly changes but the value stays in the order of 10^{-19} m^2.

The mechanical data in Fig. 8 shows that no dilatancy, but only compaction of the sample occurred with straining. Under similar testing conditions, the permeability of the mudstone rock salt is approximately 1–2 orders of magnitude higher than that of the pure rock salt, which shows that mudstone impurities might have adverse effects on the sealing performance of the rock salt. This may be deduced from two reasons: (i) the mechanical properties of grain boundaries have been changed due to the filling of impurities, which results in more difficulty for the cracks to be well compacted; and (ii) the fragile fractures of the impurities induce more pores and fissures in the sample.

Compared to the pure rock salt, the sealing performance of mudstone rock salt seems poorer. Even so, the permeability 10^{-19} m^2 is still low enough to satisfy the tightness requirement of the cavern for storing natural gas. However, the design and management of a gas storage cavern should include not only the tightness, but also the stability. Although the permeability of the mudstone rock salt is much higher than that of the pure rock salt, what we should not ignore is that the strain accommodated is much smaller. According to Figs. 6 and 7, under the same differential stress and permeant gas pressure, the peak strain of the mudstone rock salt is only 2.97%, but 6.43% of the pure rock salt. Also the volumetric strain (ε_V) is about −0.42% of the mudstone rock salt, but −1.03% of the pure rock salt. This indicates that the volume convergence of the cavern in mudstone salt strata will be

much smaller than that in pure rock salt if being operated under the same conditions of the internal gas pressure.

For the mudstone rock salt, the permeability still remains around 10^{-19} m^2 when the differential stress has been up to 40 MPa. Also, neither dilatancy nor steep increase of permeability was observed. This shows that the threshold value of deviatoric stress when a sudden change of permeability occurs is higher than 40 MPa (P_c = 20 MPa). Thus, the stability and tightness of gas caverns in such strata provides satisfactory safety reserve.

4.1.3. Discussion on the permeability evolution of the rock salt

The decrease of the permeability is mainly induced by the cracks closing, thus reducing the connectivity. For the mudstone rock salt, the damage degree induced by stress release and sample preparation is higher compared to that of the pure rock salt, and the damage of the matrix is also higher. That is why a higher permeability appears in mudstone rock salt. Therefore, the compression sensitivity of the mudstone rock salt under hydrostatic pressure is higher. On the visible and micro-scales, the impurities, consisting of fine clay minerals, polyhalites and sodium feldspar and so on, are randomly distributed among the grains of halite (as seen in Fig. 11-b). The higher the proportion of mudstone impurities, the more the properties of the boundaries of the halite grains will be influenced, and the weaker the capacity of recrystallization under compression will be. According to the different evolutions of the permeability of the pure and mudstone rock salt after unloading, the permeability of mudstone rock salt increased a little, proposing that some closed cracks re-opened again. By this phenomenon, it can be deduced that the higher the proportion of the mudstone impurities, the weaker the elastic hysteresis will be. Therefore, to maintain relatively low permeability, the internal gas pressure of a cavern located in mudstone salt strata should be lower than that in pure rock salt strata. Also, the fast withdrawal period should be shorter.

4.2. Permeability investigation on interfaces

The interface is a structure which connects the mudstone interlayer and the rock salt layer. Due to the transitional physical and mechanical properties, stress concentration and differential deformation appear near the interface. In traditional view, the interface, a structural surface, usually is a weak region of poor mechanical strength and high permeability. Therefore, many researchers are concerned whether the micro-structure and sealing performance of the interfaces in bedded rock salt can satisfy the requirements to be an effective barrier. In this paper, two typical interface samples are selected for permeability tests: horizontal interface, which corresponds to the middle location in the cavern, and inclined interface, which corresponds to the haunches of the cavern (seen in Fig. 5). These two samples are helpful for applying tensile and shearing stress during loading.

4.2.1. Permeability evolution of horizontal interface (sample 3-16-1)

Two runs of permeability tests have been conducted on the vertical interface Sample 3-16-1, the planning of the confining pressure and differential stress of the two runs are as shown in Fig. 9-b. At the beginning of the first run under confining pressure of 5 MPa, the permeability is as high as 1.10×10^{-15} m^2. Another dot of permeability is measured at the same confining pressure of 5 MPa, which is 1.51×10^{-15} m^2. Increasing the confining pressure to 20 MPa, the permeability quickly reduces to 1.07×10^{-16} m^2, the reduction proportion of which exceeds 92.8%. Afterwards, the permeability remains in the range of 1.07×10^{-16} m^2 to 4.71×10^{-17} m^2. This phenomenon is very similar with those in our previous study, that is the permeability of the mudstone decreases

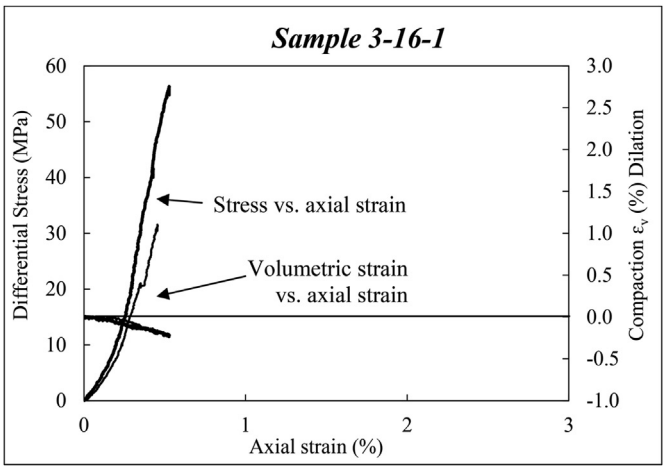

a

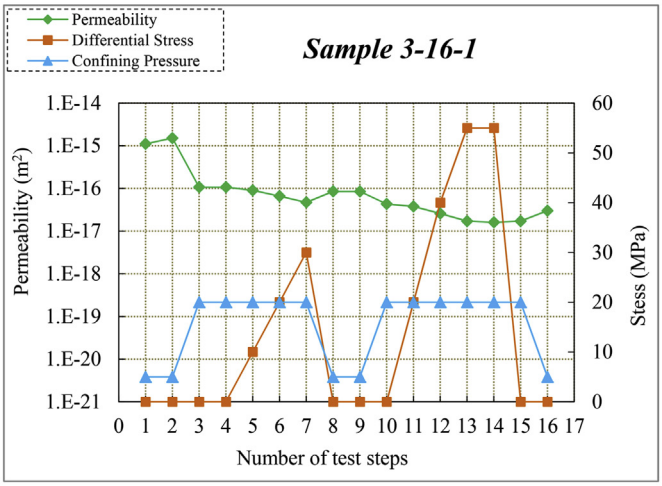

b

Fig. 9. Mechanical and permeability testing results of the vertical interface: Differential stress and volumetric strain vs. axial strain; (b) permeability (primary y-axis), confining pressure and differential stress (secondary y-axis) in sequence of steps.

very fast and then remains very stable when the hydrostatic pressure exceeds the "Compression threshold pressure" (Liu et al., 2015). It is found that there is no increase of permeability when the differential stress is 40 MPa. This supports argument that, for the interface, the threshold for the steep increase in the permeability needs a higher differential stress.

Stress concentration occurs in the regions of the interface due to the unmatched deformations in this region. To investigate how stress concentration will cause adverse effects on the permeability of the interface, a second run of the permeability tests is conducted. The differential stress is set to be in the range of 0–55 MPa (confining pressure remains 20 MPa). In this run of tests, the decrease of the permeability with the increasing differential stress is largely linear, and the final permeability has become as low as 1.61×10^{-17} m^2. In contrary to our initial expectation of the second run, the maximum differential stress is high enough that slippage or fracture will occur along the interface resulting in dilatancy and increase of permeability. However, at the end of run, dilatancy and increase of permeability still did not occur (Fig. 9). This strongly indicates that the resistance capacity to deformation and the

strength of the interface is excellent, and the cementation of the mudstone and the rock salt is very strong. In the depth range of 1000–2000 m of the gas caverns in China, the differential stress in the cavern wall rock is almost impossible to exceed 55 MPa. So for such interfaces in the wall rock, it is difficult that dilatancy and permeability of the interfaces will increase, which is favourable for the tightness and stability of the cavern.

4.2.2. Investigation on inclined interface (sample 2-3)

The Sample 2-3 contains an inclined interface connecting the rock salt part and mudstone part. The inclination angle is approximate 45°. To guide the gas to flow through the interface, two holes of 2.5 mm in diameter had been drilled in the top and bottom ends of the sample (Fig. 5). The depth of the hole on the mudstone part side is 36.9 mm, at a distance of about 16 mm radially away from the core axis; another hole was drilled in the rock salt part side, 25.4 mm in depth and 15 mm radially away from the core axis.

Keeping the entire test conditions (P_c, temperature, strain rate) constant, the permeability was measured using the same transient pulse decay method as described above. The results thus obtained show a decreasing permeability with increasing differential stress, as shown in Fig. 10-a. For this particular sample with an oblique interface, we anticipated the risk of shear fracture development at the interface, but the confining pressure (20 MPa) was high enough to suppress dilatancy and the interface remained bonded with no signs of slippage. The sample became more compacted with increasing strain, closing grain boundaries (Fig. 10-b) and reducing permeability. The permeability of the inclined interface is very low, 5.83×10^{-17} m^2. With the increase of confining pressure and differential stress, the permeability continuously decreases to 6.21×10^{-18} m^2. The reduction is much smaller than those of the rock salt samples, indicating that little damage is induced on the interface region. During the unloading process, the end permeability has increased to 2.24×10^{-17} m^2, approximately 3.5 times of the lowest value in this sequence. It shows that the deformation of the sample is partially elastic, thus the micro-cracks rebounded and resulted in a rising permeability during the unloading stage.

4.2.3. Discussion on the permeability evolution at interface

According to the above study on the permeability evolution of the interface, two basic properties of the interfaces can be deduced: (1) the permeability of the interface is higher than those of the mudstone and rock salt, but its value always remains around the order of 10^{-17} m^2, still belonging to low permeable media; (2) the cementation at the interface is very strong and hence there is no sharp increase of permeability even when the differential stress is high.

The permeability evolution of the vertical interface is similar to that of the mudstone in our previous study, which is that the permeability decreases very fast and then becomes stable once the hydrostatic pressure exceeds the 'Compression threshold pressure' (Liu et al., 2015). The mechanical data suggest that the deformation is mostly elastic and the major proportion of the applied load is undertaken by the mudstone half to keep deformation equipment, because the mudstone has a much greater modulus than that of the rock salt. The sample was carefully studied after the experiment for mechanical damage, and no fracture was found. But after a couple days, two cracks appeared on the mudstone part, which might be due to delayed degassing of the sample and/or elastic incompatibility at the interface.

4.3. Measurements of microscopic structures and components

Permeability is an effective way on the macroscale to indicate the hydraulic properties of the bedded salt rocks. But it is not enough to completely investigate the mechanism of the low permeability characteristics of the bedded salt rocks. As a supplement to further interpret the hydraulic properties of the rocks, SEM and EDS (Energy Dispersive Spectrometer) tests have been conducted.

The sample of each lithotype of the bedded rock salt used for SEM is taken from the same cores as for the above permeability testing samples. The electron microscope used in this study is Phenom Prox, which is capable to get the microscopic-images and the element components at the same time. The results of pure and mudstone rock salt are shown in Fig. 11.

Fig. 11-a shows that the crystals of the pure rock salt are closely packed and the matrix looks tight. Rock salt has typically composite crystalline structure, even enlarged 2000 times, there are still visible crystal boundaries, but these boundaries are tightly closed. From the above images in Fig. 11-a, the microscopic-structure of the rock salt is very tight, that is why pure rock salt has extremely low permeability and excellent tightness. As seen in Fig. 11-a, EDS results shows that the pure rock salt contains mainly halite and a little impurities, such as organic matters. Numerous very small halite

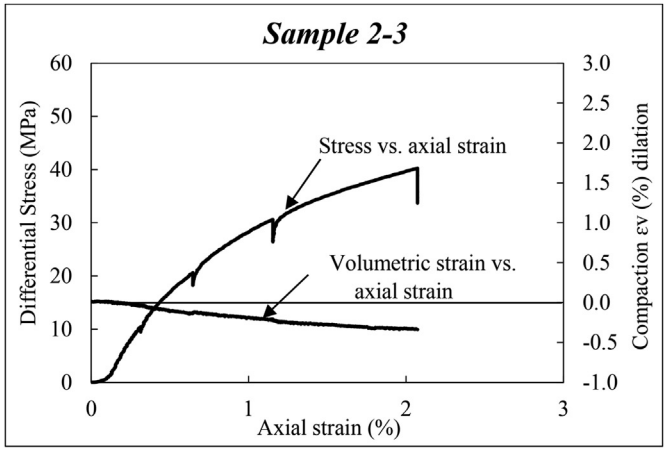

a

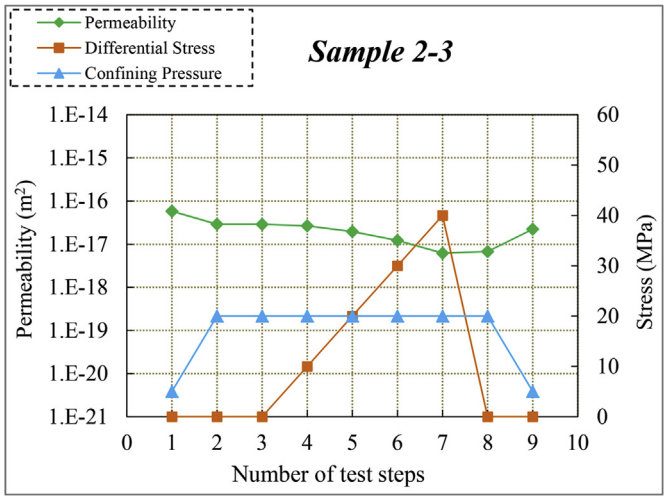

b

Fig. 10. Mechanical and permeability testing results of the inclined interface: Differential stress and volumetric strain vs. axial strain; (b) permeability (primary y-axis), confining pressure and differential stress (secondary y-axis) in sequence of steps.

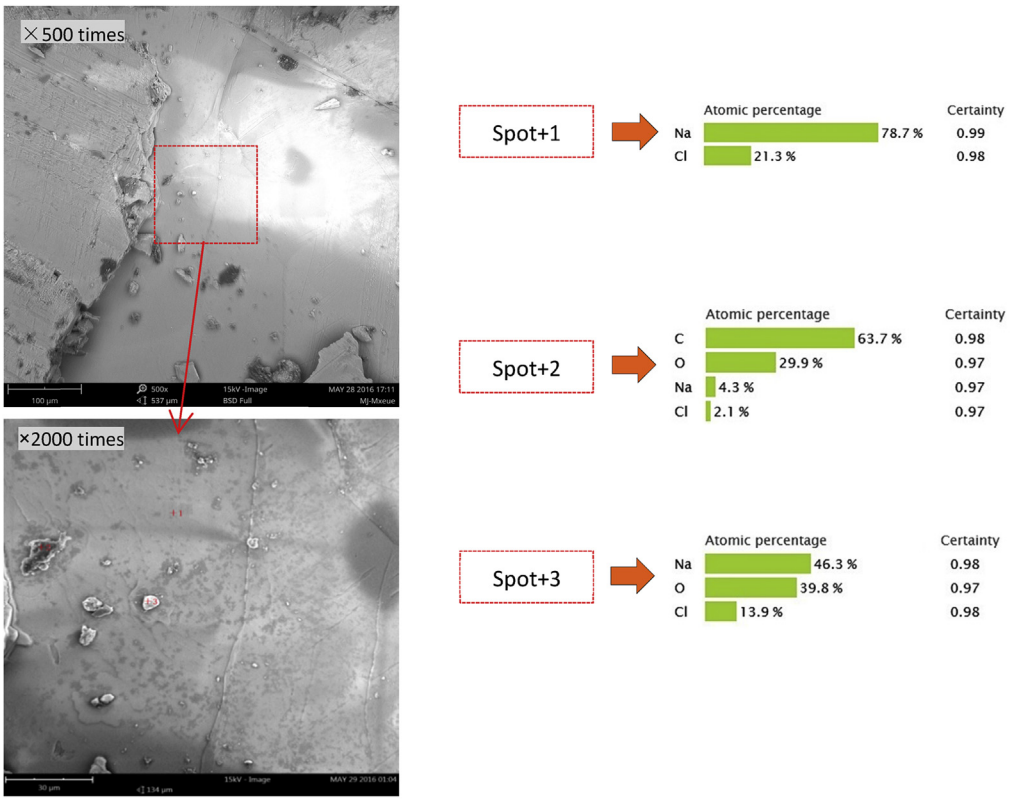

a Typical SEM and EDS results of pure rock salt

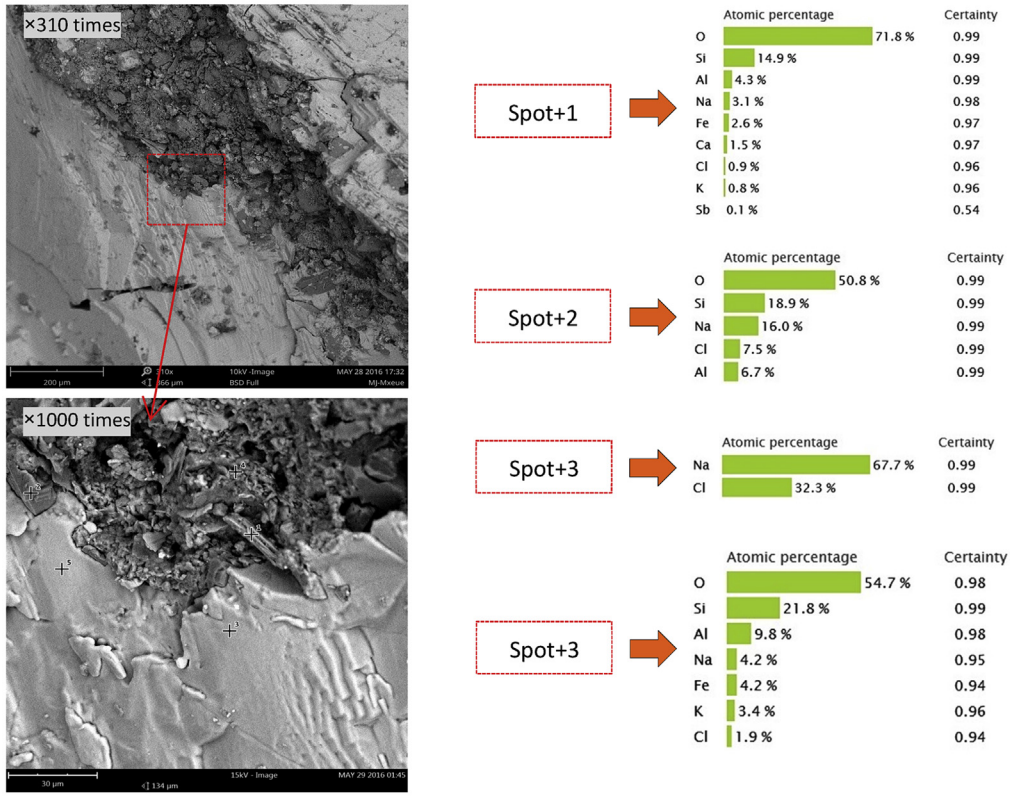

b Typical SEM and EDS results of mudstone rock salt

Fig. 11. The results of the SEM and EDS measurements by Phenom Prox.

grains accumulate on the surface of large crystals.

For the more common grey-black impure rock salt, both the microscopic images and the EDS results are shown in Fig. 11-b. As of the image with a magnification of 310 times, the impurities forms a band locating in between halite crystals, as the image in upper-left shows. With further enlarging the image to 1000 times, clearer structure and combination of impurities and halite crystals are obvious. As seen in the low-left image of Fig. 11-b, the halite rich part is very tight with almost no cracks or voids. As the transition region, halite crystals and the impurities are tightly connected with an uneven interface, not a discontinuous region with an aperture. As of the impurities rich part, numerous voids are seen. However, the diameters of the voids are mostly less than 5 μm. Such a small size of the voids is so small that it will help a certain to the pressure and discourage the gas to flow through.

In a word, the tightness of both the pure and the mudstone rock salt are good to excellent. And the microscopic structure of the pure rock salt performs to be a satisfactory to perfect seal. Micro-voids exists in impurities rich part, so the tightness degree of the impure rock salt is poor than that of the pure rock salt. This is why the pure rock salt has lower permeability than the impure rock salt.

5. Numerical simulation of the gas seepage around the cavern

5.1. Determination of permeability values

a) Permeability of the interlayer

Referring to our previous work (Liu et al., 2015): the permeability of the mudstone interlayer is as high as 10^{-16} m^2 if the confining pressure is very low (such, approximately 2 MPa); whereas, when the confining pressure increases in the range of 2–5 MPa the permeability rapidly reduces by about 2 orders of magnitude, and then remains very stable. The authors indicated that the reason for decrease of the permeability is related to the stress relaxation of cores during drilling, the damage induced by sample preparation and the samples drying before test, which caused the micro-cracks to reopen and connect, thus resulting in the higher permeability under low confining pressure. By increasing the confining pressure, the cracks reclosed and the connectivity decreased, and the permeability rapidly decayed. For the interlayer intersecting the cavern wall, although cavern leaching causes a certain stress relaxation, mechanical damage or cracks connecting, the wall rock are still under well-compressed state, thus the permeability of the interlayers should adopt the value when exceeding the compressive threshold confining pressure (Liu et al., 2015). Thus, in the present study, the permeability of mudstone interlayer (κ_{IT}) is valued as 5×10^{-18} m^2 for simulation studies.

b) Permeability of the interface

The permeability of the interfaces decreases linearly with the increase of the confining pressure and deviatoric stress. Even when the deviatoric stress is very high, the trend does not change. However, the variation is small, always around 10^{-17} m^2. Although the permeability of the interface is about one order of magnitude higher than that of the interlayer, and 2 to 3 orders of the rock salt, strictly considering the absolute value, 10^{-17} m^2, it still belongs to low permeable rocks (Chen et al., 2009). Even so, it is notable that gas seepage along the interface will be much faster than those in the interlayers and salt layers. In this study, for exercise, we set the intermediate value of the permeability of the interface (κ_{IF}) as 5×10^{-17} m^2 for simulation studies.

c) Permeability of the rock salt

For rock salt, it is also found that the initial permeability is very high. However, the salt cavern leaching time lasts approximately 4–5 years (Yang et al., 2009), such a long time is enough for the damage of the rock salt to self-heal, provided the salt is wet enough (Houben et al., 2013). So the permeability of rock salt should be of the orders of value when it is well-compressed. From the aforementioned studies, it is found that the permeability of the pure rock salt is lower than 10^{-21} m^2 after the sample is well-compressed; and even for mudstone rock salt (high proportion of impurities), the permeability of which still lowers to 10^{-19} m^2. In this study, the highest impurities proportion of the rock salt is close to 30%. Therefore, the permeability of the rock salt should be in range between 10^{-19} m^2 and 10^{-21} m^2. Considering the strict safety demand of natural gas storage cavern, we set the permeability of the rock salt (κ_{salt}) as 1×10^{-19} m^2 for safer designing.

5.2. Numerical simulation model

The cavern is designed as an ellipsoid, with horizontal diameter of 70 m and vertical height of 120 m. There are 3 main mudstone interlayers in the cavern sections, with thickness of 2.5–3.5 m. The interface is set as a layer with a thickness of 0.3 m. A typical finite differential element simulator, FLAC^{3D} (Itasca, 2005) is used to establish the 3D-geomechanical numerical model. This model has a length of 480 m, a thickness of 170 m and a height of 440 m. Due to symmetry of the model, one one-half of the cavern is established and located at the centre of the front face. The sizes of left and right side are both larger than 6 times of the cavern radius (240 m > 6 × 35 m = 210 m), thus such a size satisfies the seepage boundary. In height direction, due to the seals of top salt layer and bottom salt layer, gas has a small possibility to migrate into the upper and lower mudstone layers, so the mudstone layers in upper and lower locations are 170 m and 150 m respectively, a little thinner than that of the transverse surrounding rocks. Considering that the surrounding rocks near the cavern are the main seepage regions, the element size has been meshed with small size to improve the simulation efficiency; whereas the farer elements are meshed with larger sizes to improve calculation rate. Upper the top face of the model, the gravity force of the upper strata has been simplified as the surface force on this face to reduce the amount of calculation. The other five faces are set as the impermeable boundaries of the model, and are all displacement constraint. The entire model has 60,840 zones and 67,025 grids in total. The established model is as Fig. 12 shows.

5.3. Gas seepage and tightness assessment

5.3.1. Gas seepage in entire rock wall

In general, the mean value of the operational internal gas pressure is designed to be a little higher than half of the gravity stress at the middle location of the cavern. Thus, we set an internal gas pressure of 13 MPa and simulated a lifespan of 30 years to simulate the gas seepage in the vicinity of the cavern. The gas seepage around the cavern during 10 years–30 years was illustrated in Fig. 13. According to Fig. 13, the seepage distance in the interface ($\kappa_{IF} = 5 \times 10^{-17}$ m^2) is the largest compared with those in interlayers and in rock salt. Although the permeability of the interlayer ($\kappa_{IL} = 5 \times 10^{-18}$ m^2) is one order of magnitude lower than that of the interface, the seepage distance and the pore pressure in the interlayer is only a little smaller than those in the interface. This also shows that the permeability of the interface influences much the gas seepage around the cavern, in particular the seepage in the adjacent interlayer. As for the rock salt, except for a small seepage

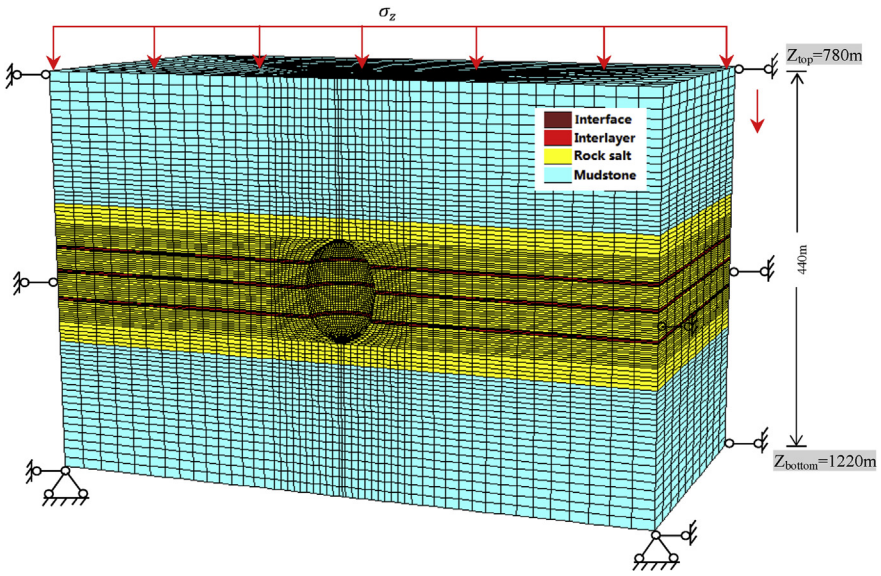

Fig. 12. Schematic of the 3D-numerical model for a single cavern in bedded salt rocks (the numbers of the interlayers from up to down are 1–3, and 1 to 6 of the interfaces).

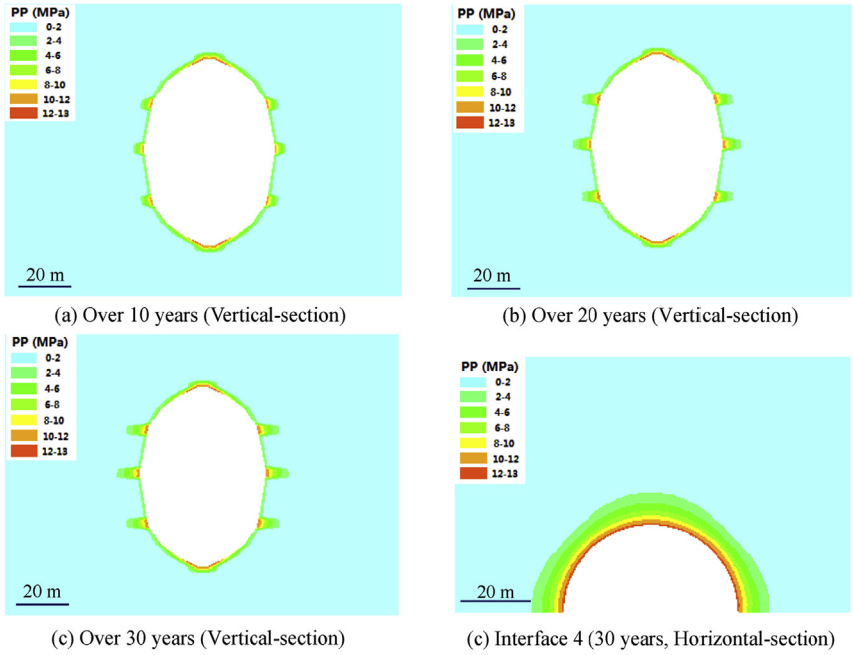

(a) Over 10 years (Vertical-section)

(b) Over 20 years (Vertical-section)

(c) Over 30 years (Vertical-section)

(c) Interface 4 (30 years, Horizontal-section)

Fig. 13. Gas seepage evolution around the cavern over 30 years.

distance in the roof and bottom of the cavern, the seepage is almost invisible in other regions. High seepage pressure appears in the interfaces and interlayers, but their regions are very small and at most cause only a small region of local failure on the cavern surface. In the whole, the seepage rate is very slow and the seepage distances in the vicinity of the cavern are also very small, so the tightness of the wall rock of the cavern is favourable.

For a further and quantitative interpretation of the seepage evolutions in different strata around the cavern, the seepage distance versus operating time has been plotted in Fig. 14. From Fig. 14, in the three different strata, the seepage distances increase as operational time goes on, but the rate of increase is fast at the initial stages and then gradually reduces. The seepage distance is the largest in the interface, about 15.72 m over 30 years. The seepage distance in the interlayer is only a little shorter (0.5–1.0 m) than that in the interface. In the rock salt the seepage distance is always less than 3 m even when operating over 30 years, causing almost no effect on the tightness of the cavern.

Generally, there is a complex distribution of caverns in underground space. Pillar width between adjacent caverns is an important parameter and should be designed by comprehensively considering the stability and tightness. Wang et al. (2015b) recommended that the pillar width should be at least 1.5 times the cavern diameter and the pore pressure at the middle point of the pillar should be lower than the lowest internal pressure to ensure the tightness of the pillar. As seen in the above study, the seepage distance along the interface is only 15.72 m and is only 15% of the smallest pillar width (1.5×70 m $= 105$ m). If the caverns are

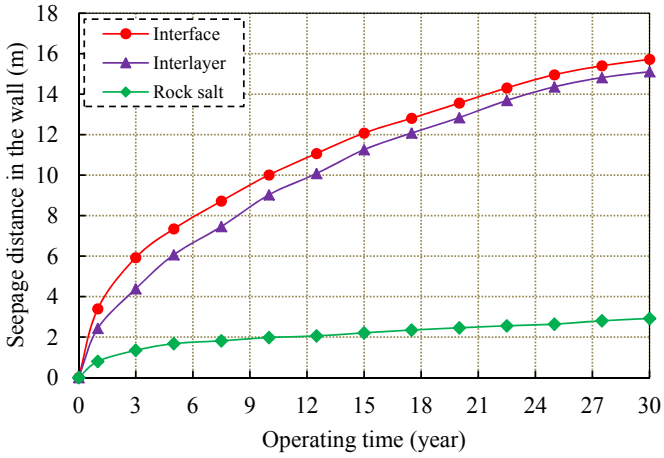

Fig. 14. Seepage distance as a function of operating time in different stratum.

constructed in the bedded rock salts as we studied in this work, such a small seepage distance is far from the middle point of the pillar, let alone causing pore pressure in this zone. Therefore, it is deduced that the seepage along the interface has very small influence on the stability of the wall rock.

5.3.2. Sensitivity analysis for several factors

In fact, the tightness of the cavern is influenced by many aspects, such as the internal gas pressure, locations of the interface, and the permeability of the interlayer, etc. To indicate how these factors will influence the tightness of the cavern, the sensitivity of these factors are analyzed in this section as follows:

i) Effect of the internal gas pressure

The internal gas pressure of a cavern is variable, and reasonably designing the pressure of the internal gas is an important task for the management of the natural gas storage. Five internal gas pressures (9–17 MPa) have been simulated to investigate how gas seeps around the cavern for each case. The operating time is also 30 years, and the other conditions are the same as above. As the interface is the most important structure which controls the gas seepage and tightness of the cavern, we still focus on the seepage in the interface-4. The seepage distance versus the pore pressure under each pressure is depicted in Fig. 15 after operating for 30 years.

As shown in Fig. 15, the pore pressure reduces fast in nearer regions and gradually becomes stable in farther regions. For higher internal gas pressure, the pore pressure is higher at the same location. From the viewpoint of tightness, lower gas pressure is advantageous, for both the pore pressure and the seepage distance will be smaller in the rock wall. But it is adverse for the stability of the cavern, because lower gas pressures are incapable to restraining the convergence of the cavern or to store larger amount of gas. On the other hand, a too high gas pressure is also not adoptable, for it might cause high pore pressure accumulating in the wall rock and exerts adverse impacts on the stability of the cavern. Thus, a reasonable range of the gas pressure should be considered, taking into account the stability, tightness, pillar width, and internal pressure conditions.

ii) Effect of the interface location

Interfaces can be situated at different locations intersecting the cavern. To reveal how gas migrates to different locations of the interlayer, the seepage distance versus the pore pressure along Interfaces 2, 4 and 6 has been plotted, as shown in Fig. 16. The pore pressure along different surfaces versus seepage distance is very similar. The location has only a little influence on the seepage evolution along the interface.

iii) Effect of the interlayers' permeability

According to our previous studies, the interlayers contain mudstone, glauberite and grey clay, the permeability of which is in the range of the 10^{-18} m^2 to 10^{-20} m^2 (Liu et al., 2015). To demonstrate how the permeability of the interlayers affects the gas seepage and tightness around the cavern, four values of the permeability of the interlayer are set: $\kappa_{IL1} = 5 \times 10^{-18}$ m^2, $\kappa_{IL2} = 1 \times 10^{-18}$ m^2, $\kappa_{IL3} = 5 \times 10^{-19}$ m^2, $\kappa_{IL4} = 1 \times 10^{-19}$ m^2. Fig. 17 shows how the seepage distance versus the pore pressure along the Interface-4 when the interlayers have different permeabilities. When the permeability of the interlayers is higher, the seepage distances along the interface and in the adjacent interlayer are almost the same. As the permeability of the interlayer reduces, the seepage distance gradually decreases. The study shows that when the ratio of the interlayer's permeability to the interface' permeability is in the range of 0.01–0.1, the migration rate in the interlayer lags only a little behind that in the interface; whereas, when

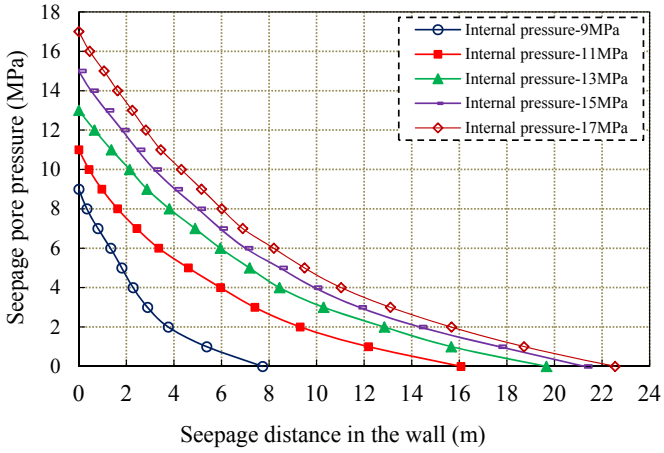

Fig. 15. Seepage distance as a function of seepage pore pressure over 30 years (in Interface-4).

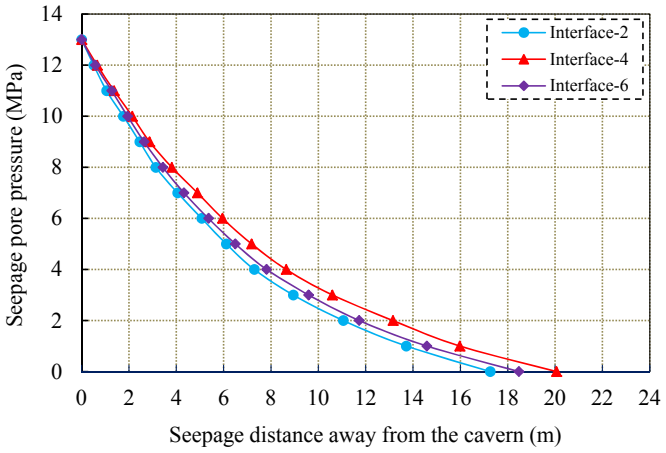

Fig. 16. Seepage pore pressure along different interfaces versus seepage distance over 30 years.

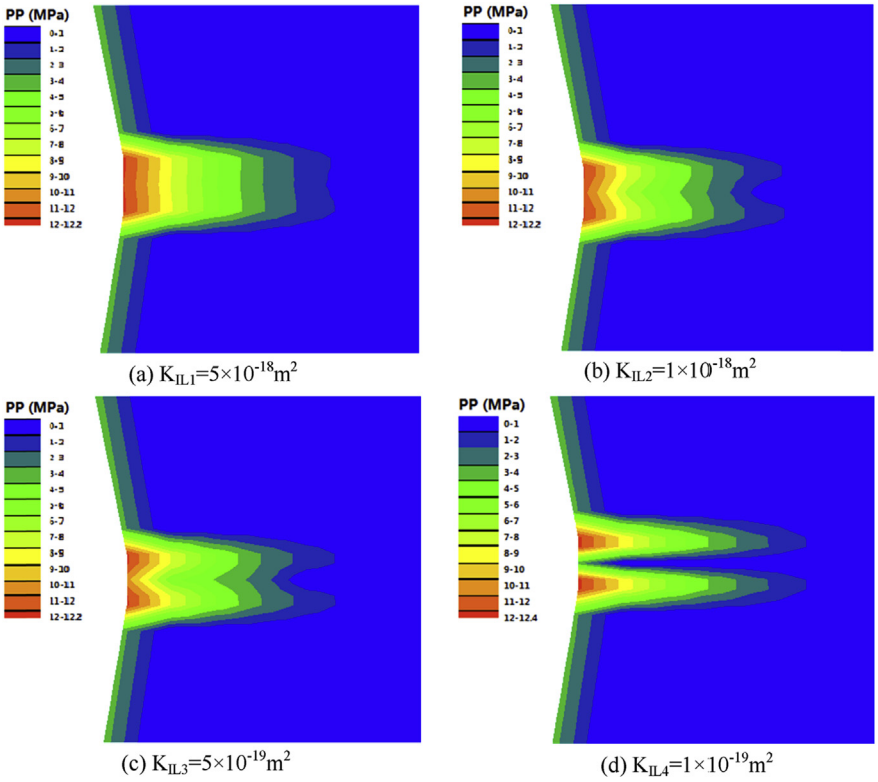

Fig. 17. Gas seepage around the interfaces and interlayer when the interlayer has different permeabilities (IL is short for Interlayer) over 30 years.

the permeability of the interlayer is lower to 1×10^{-19} m^2, the seepage in the interlayers becomes very small and the main seepage appears in the interfaces. When the interlayers have different permeability, the migration rate of the gas in the interface seems almost invariant.

5.4. Overall evaluation of the tightness

In the current studies, it is demonstrated that an interface is a key structure to influence the gas seepage in the vicinity of the cavern. When the interface has high permeability, the seepage distance will be large and the pore pressure will be high. Large seepage distance and high pore pressure will also be induced in the adjacent interlayer. Internal gas pressure and permeability of interface have a notable influence on the seepage distance and the pore pressure; the location of the interface has little effect. The gas seepage influences only a small range around the cavern, so the tightness of the gas storage cavern in such bedded salt formation is satisfactory.

6. Conclusions and prospects

Laboratory measurements of the permeability and mechanical properties have been conducted for the first time on bedded rock salts cores from a pilot-well in Jintan Salt Mine, Jiangsu Province, China. Based on the laboratory results, the gas seepage in the vicinity of a natural gas cavern in this bedded salt beds is numerically simulated to evaluate the tightness of the cavern. Several conclusions from this study are presented as follows:

(1) The permeability of the bedded rock salt is in the range of 10^{-17}–10^{-21} m^2, extremely low permeability media. The permeability of the rock salt reduces to 10^{-19} to 10^{-21} m^2 when subjected to high confinement and deviatoric stress. The pure rock salt even behaves as an impermeable material ($<10^{-21}$ m^2) and shows excellent plastic capacity during loading and unloading; mudstone rock salt has a higher permeability, around the order of magnitude of 10^{-19} m^2, for the flexible deformation capacity of which is poorer than that of the pure rock salt.

(2) The permeability of the interface is always around the order of magnitude 10^{-17}–10^{-18} m^2, belonging to lower permeable media but the variation range is much less than that of the rock salt. Even under very high deviatoric stress, both dilatancy and consequent increase of permeability did not occur, which indicates that the texture of the interface is of strong cementation and tight microstructure. These properties of the interface are favourable for the tightness and stability of gas cavern in such a bedded salt formation. Combined with our previous study (Liu et al., 2015), the measurements of SEM show tight microstructure of the bedded rock salt, a supplement to support the evidence for the satisfactory tightness of the target salt beds.

(3) The numerical simulation results of the gas seepage indicate that the interfaces are the predominant channels for the gas to infiltrate through. Along the interface, the gas seeps the fastest and the pore pressure increases the most. When the permeability of the interlayer is 1–2 orders of magnitude greater than that of the interface, the seepage distance in the interlayer is slightly different from those in adjacent interfaces. As a whole, the seepage in the rock salt is too slow to cause any remarkable effect on the tightness of the cavern wall.

Comprehensively evaluating the tightness of the gas cavern in the bedded salt formations in terms of the permeability

characteristics, the evolution of the permeability with the deviatoric stress, as well as the gas seepage around the cavern, the bedded rock salt is satisfactory for the tightness requirements of the natural gas storage cavern situated in.

Acknowledgement

The authors would gratefully like to acknowledge the financial support from the National Natural Science Foundation of China (No.41472285, 51574048, 51304256, 51604044, 41672292), the China Postdoctoral Science Foundation (No.2015M582520, 2015T80857), the Doctoral Program of Higher Specialized Research Fund (20130191130003), the support from the Fundamental Research Funds for the Central Universities (No.106112016CDJCR241219, No.106112016CDJZR245518) the visiting scholar funded project of the State Key Laboratory of Coal Mine Disaster Dynamics and Control (Chongqing University) (No.2011DA105287-FW201401) and the International Cooperation Project of Sichuan Province (No. 2014HH0007).

References

Alkan, H., 2009. Percolation model for dilatancy-induced permeability of the excavation damaged zone in rock salt. Int. J. Rock Mech. Min. Sci. 46 (4), 716–724.

Brace, W.F., Martin, R.J., 1968. A test of the law of effective stress for crystalline rocks of low porosity. Int. J. Rock Mech. Min. Sci. Geomech. Abstr. 5 (5), 415–426.

Chen, W.Z., Tan, X.J., Wu, G.J., Yang, J.P., Wu, G.J., Yang, J.P., 2009. Research on gas seepage law in laminated salt rock gas storage. Chin. J. Rock Mech. Eng. 2009 (7), 1297–1304 (in Chinese).

Consenza, P., Ghoreychi, M., Bazargan-Sabet, B., Marsily, G.D., 1999. In situ rock salt permeability measurement for long term safety assessment of storage. Int. J. Rock Mech. Min. Sci. 24, 509–526.

Hou, Z.M., 2003. Mechanical and hydraulic behavior of rock salt in the excavation disturbed zone around underground facilities. Int. J. Rock Mech. Min. Sci. 40 (5), 725–738.

Houben, M., Hove, A.T., Peach, C.J., Spiers, C.J., 2013. Crack healing in rocksalt via diffusion in adsorbed aqueous films: microphysical modelling versus experiments. Phys. Chem. Earth 64, 95–104.

Hunsche, U., 1996. Determination of the Dilatancy Boundary and Damage up to Failure for Four Types of Rock Salt at Different Stress Geometries. In: Proceedings of the 4th Conference on the Mechanical Behavior of Salt, 1996. Trans Tech Publications, Montreal, pp. 163–174.

International Energy Association, 2012. Natural Gas Information 2012. http://www.iea.org/media/training/presentations/statistics march/Natural Gas Information.pdf.

Itasca, 2005. FLAC3D Version 3.0 Manual. Itasca Consulting Group, Inc., Minneapolis.

Johnson, D.O., Seni, S.J., 2011. Regulation of hydrocarbon storage operations in Texas. In: Proc SMRI Spring Meeting, Orlando, 2001, pp. 111–120.

Jong, C.D., 2015. Gas storage valuation and optimization. J. Nat. Gas. Sci. Eng. 24, 365–378.

Klinkenberg, L.J., 1941. The permeability of porous media to liquids and gases. Socar Proc. 2 (2), 200–213.

Li, Y.P., Yang, C.H., Daemen, J.J.K., Yin, X.Y., Chen, F., 2012. A new Cosserat-like constitutive model for bedded salt rocks. Int. J. Numer. Anal. Meth. Geomech. 33, 1691–1720.

Li, Y.P., Liu, W., Yang, C.H., Daemen, J.J.K., 2014. Experimental investigation of mechanical behaviour of bedded rock salt containing inclined interlayer. Int. J. Rock Mech. Min. Sci. 69 (3), 39–49.

Liu, W., Li, Y.P., Yang, C.H., Daemen, J.J.K., Yang, Y., Zhang, G.M., 2015. Permeability characteristics of mudstone cap rock and interlayers in bedded salt formations and tightness assessment for underground gas storage caverns. Eng. Geo. 193, 212–223.

Muhammad, N., Spiers, C.J., Peach, C.J., Bresser, J.H.P.D., Liu, W., 2015. Permeability of layered rock salt at different stresses and geometries. In: Roberts, Mellegard, Hansen (Eds.), Mechanical Behavior of Salt VIII. CRC Press, pp. 23–33.

Peach, C.J., Spiers, C.J., 1996. Influence of crystal plastic deformation on dilatancy and permeability development in synthetic salt rock. Tectonophysics 256 (s 1–4), 101–128.

Staudtmeister, K., Rokahr, R.B., 1997. Rock mechanical design of storage caverns for natural gas in rock salt mass. Int. J. Rock Mech. Min. Sci. 34 (3–4), 300.e1–300.e13.

Stormont, J.C., 1997. In situ gas permeability measurements to delineate damage in rock salt. Int. J. Rock Mech. Min. Sci. Geomech. Abstr. 34 (7), 1055–1064.

Walder, J., Nur, A., 1986. Permeability measurement by the pulse-decay method: effects of poroelastic phenomena and non-linear pore pressure diffusion. Int. J. Rock Mech. Min. Sci. Geomech. Abstr. 23 (3), 225–232.

Wang, T.T., Ma, H.L., Yang, C.H., Shi, X.L., Daemen, J.J.K., 2015a. Gas seepage around bedded salt cavern gas storage. J. Nat. Gas. Sci. Eng. 26, 61–71.

Wang, T.T., Yang, C.H., Yan, X.Z., Daemen, J.J.K., 2015b. Allowable pillar width for bedded rock salt caverns gas storage. J. Petro. Sci. Eng. 127, 433–444.

Xiong, J., Huang, X.L., Ma, H.L., 2015. Gas leakage mechanism in bedded salt rock storage cavern considering damaged interface. Petroleum 1 (4), 366–372.

Yang, C.H., Li, Y.P., Chen, F., 2009. Bedded Salt Rock Mechanics and Engineering. Science Press, Beijing (in Chinese).

Yang, C.H., Wang, T.T., Li, Y.P., Yang, H.J., Li, J.J., Xu, B.C., et al., 2015. Feasibility analysis of using abandoned salt caverns for large-scale underground energy storage in China. Appl. Energy 137, 467–481.

Yang, Y.L., Aplin, A.C., 2010. A permeability–porosity relationship for mudstones. Mar. Pet. Geo. 27 (8), 692–697.

Zhang, G.M., Li, Y.P., Yang, C.H., Daemen, J.J.K., 2014. Stability and tightness evaluation of bedded rock salt formations for underground gas/oil storage. Acta Geotech. 9 (1), 161–179.

Zhou, H.W., He, J.M., Wu, Z.D., 2009. Permeability and meso-structure characteristics of bedded salt rock. Chin. J. Rock Mech. Eng. 28 (10), 2068–2073 (in Chinese).